ELSEVIER

Chemical Engineering Journal 143 (2008) 124–132

Chemical Engineering Journal

www.elsevier.com/locate/cej

Effects of the operating parameters on the production of bio-oil in the fast pyrolysis of Japanese larch

Hyun Ju Park [a], Jong-In Dong [a], Jong-Ki Jeon [b], Young-Kwon Park [a,*], Kyung-Seun Yoo [c], Seung-Soo Kim [d], Jinsoo Kim [e], Seungdo Kim [f]

[a] *Faculty of Environmental Engineering, University of Seoul, 90 Jeonnong-Dong, Dondaemun-Gu, Seoul 130-743, Republic of Korea*
[b] *Department of Chemical Engineering, Kongju National University, 182 Sinkwan-Dong, Gongju, Chungnam 341-701, Republic of Korea*
[c] *Department of Environmental Engineering, Kwangwoon University, 447-1 Wolgye-Dong, Nowon-Gu, Seoul 139-701, Republic of Korea*
[d] *Research Center, Korea Institute of Petroleum Quality, 653-1, Yangcheong-ri, Ochang, Cheongwon, Chungbuk 363-883, Republic of Korea*
[e] *College of Environment & Applied Chemistry, Kyung Hee University, 1 Socheon-Dong, Giheung-Gu, Yongin, Gyeonggi 449-701, Republic of Korea*
[f] *Department of Environmental Sciences and Biotechnology, Hallym University, 1 Okchon-dong, Chuncheon, Gangwon-do, Republic of Korea*

Received 11 August 2007; received in revised form 28 December 2007; accepted 28 December 2007

Abstract

This study examined the kinetics of the pyrolysis of Japanese larch using thermogravimetric analysis (TGA), and fast pyrolysis with a bubbling fluidized bed reactor and a two-staged char removal system under various reaction conditions. The effects of the reaction conditions on the chemical and physical characteristics of bio-oil were also examined. Japanese larch was decomposed at temperatures ranging from 250 to 380 °C. The apparent activation energies ranged from 220 and 1009 kJ mol^{-1} when the pyrolytic conversion increased from 5 to 95%. The optimal reaction temperature for the production of bio-oil was 450 °C. The bio-oil yield decreased with decreasing feed size due to overheating. The bio-oil yields increased gradually with increasing flow rate and feeding rate but these increases were not significant. The use of the product gas as the fluidizing medium was effective for the production of bio-oil, giving the highest bio-oil yield of 64 wt%, but the introduction of oxygen had a slightly negative effect on the bio-oil yield. In addition, high-quality bio-oil, which contains <0.005 wt% solid, no ash, and low concentrations of alkali and alkaline earth metals, could be produced using the two-staged char removal system. With the exception of the reaction temperature and partial oxidation, the other pyrolysis conditions did not significantly affect the chemical and physical characteristics of bio-oil.

Keywords: Kinetics; Fast pyrolysis; Japanese larch; Char removal system; Pyrolysis conditions

1. Introduction

Biomass is unique in providing the only renewable source of fixed carbon, which is an essential ingredient for meeting many of the requirements of fuel and consumer goods [1]. In addition, biomass is considered to be a readily available and sustainable energy source, with the potential to provide 11% of the world's total primary energy supplies [2].

Biomass conversion technologies can be divided into two pathways: biochemical (fermentation and anaerobic digestion) and thermo-chemical (combustion, gasification, and pyrolysis). Compared with other available biomass conversion technologies, fast pyrolysis is the least developed but offers the benefits of a liquid fuel, so called bio-oil. Bio-oil has the advantages of easy storage and transport as well as a higher power generation efficiency than fossil fueled systems at the smaller scales of operation that are likely to be realized from bioenergy systems [1]. In addition, bio-oil can be used as a feedstock in conventional petroleum refineries as well as for the production of high value chemicals.

A number of studies examined the most suitable pyrolysis conditions (e.g. temperature, feed size, sweep gas velocity, atmosphere, heating rate, steam velocity, and initial moisture content) on the production of bio-oil [3–8]. However, most studies focused on pyrolysis in a fixed bed, which is difficult to apply on a large scale. Therefore, there is a need to examine fast pyrolysis using a fluidized bed, which has high mass transfer and heat transfer rate. There is a defect in fast pyrolysis systems. Because most fast pyrolysis systems have employed cyclones only for the removal of char and ash, some fine char is inevitably carried over,

* Corresponding author. Tel.: +82 2 2210 5623; fax: +82 2 2244 2245.
E-mail address: catalica@uos.ac.kr (Y.-K. Park).

1385-8947/$ – see front matter © 2008 Elsevier B.V. All rights reserved.
doi:10.1016/j.cej.2007.12.031

resulting in catalyzing secondary cracking in the vapor phase. Even char in cooled collected bio-oil reduces its stability, accelerating the slow polymerization processes, which manifested as increasing viscosity [9]. In particular, alkali and alkaline earth metals retained mainly in char in bio-oil catalyze more of these reactions, significantly reducing its stability. In order to solve these problems, a pyrolysis system configuration applicable to the practical pyrolysis process is essential, and the experimental data related to it would provide useful information for the easier control of the pyrolysis system. In this study, the fast pyrolysis system was rearranged, with the introduction of an efficient char removal system, which consists of a cyclone and a hot filter.

More than 50% of wood wastes generated in Korea are treated by landfill and incineration, which causes significant environmental pollution. Fast pyrolysis might be an alternative not only to solve this problem but also to convert the wood wastes into the valuable product such as bio-oil. In addition, a study on kinetics of biomass decomposition as well as the reaction processes in fast pyrolysis will help control the pyrolysis reaction.

This study examined the pyrolysis of Japanese larch, which is one of the representative species in woody biomass in Korea. The global kinetic parameters were determined. The effects of various reaction conditions, such as the reaction temperature, feed size, flow rate, feeding rate, fluidizing medium, and partial oxidation on the product distribution as well as the chemical and physical characteristics of bio-oil in the fast pyrolysis of Japanese larch, were also investigated using a bubbling fluidized bed reactor, with a two-staged char removal system.

2. Experimental

2.1. Biomass

Japanese larch is used mainly in Korea as a construction and furniture material. To obtain the sawdust particle sizes for use in these experiments, the Japanese larch sawdust was screened using standard sieves with sizes ranging from 0.2 to 0.425 mm, 0.425 to 1.0 mm, and 0.85 to 1.18 mm, and was then dried in an oven (J-NDS1, JISICO) at 110 °C for 24 h to minimize the water in the oil product. After drying, the water content in the Japanese larch sawdust was <1 wt%. Table 1 lists the characteristics of the Japanese larch.

Table 1
Characteristics of Japanese larch

Chemical composition (wt%)		Proximate analysis (wt%)	
Cellulose	58.6	Water	8.8
Hemicellulose	13.0	Combustibles	91.0
Lignin	20.1	Ash	0.2

Ultimate analysis (wt%)		Alkali and alkaline earth metals (ppm)	
C	50.8	Na	92.1
H	6.8	Mg	103.3
N	0.1	Ca	529.5
O	42.4	K	348.1
S	–		–

2.2. Thermogravimetric analysis

To investigate the pyrolysis temperature range and the decomposition characteristics of Japanese larch, thermogravimetric analysis (TGA) was carried out using a thermogravimetric analyzer [TGA (TGA 2050, TA Instruments)], in a nitrogen atmosphere, at heating rates of 5–20 °C/min.

2.3. Pyrolysis apparatus

The fast pyrolysis of Japanese larch sawdust was carried out in a bubbling fluidized bed reactor. Fig. 1 shows a schematic diagram of the pyrolysis apparatus. The two-staged char removal system, which consisted of a cyclone and a hot filter, was installed consecutively at the latter part of the main pyrolysis reactor. The reactor was made from a sus-306 stainless-steel tube with a height of 300 mm and an 80 mm internal diameter. The reactors and pre-heater were heated indirectly electrically. A coiled heating tape was also used to avoid the vapor condensation in the product gas stream tube and the char removal system, which was maintained at a temperature of 400 °C. Condensable bio-oil was collected in a series of glass condensers cooled to a temperature of −25 °C using a circulator (RW-2025G, JEIO TECH) with ethyl alcohol as the cooling solvent. The non-condensable vapors that passed through the condensation system were recovered in the form of tar in an electrostatic precipitator. The pyrolysis gases through the electrostatic precipitator were sampled using Teflon gas bags at 20 min intervals to analyze their composition.

2.4. Pyrolysis conditions

The experiments were carried out above the flow rate of the minimum-bubbling fluidizing velocity (U_{mb}), and the data was analyzed using Geldart and Abrahamsen's equation [10]. Emery (NANKO ABRASIVES, Japan) with a mean 40 μm particle size was used as the bed material, and the static bed height was 0.13 m. The experimental system was purged with inert nitrogen, which as used as the fluidizing medium, for approximately 3 h before the experiments. In order to decrease the amount of heat loss during the experiments, the fluidizing gas was pre-heated to 350 °C, and introduced to the pyrolysis reactor. The temperatures of the experimental system were adjusted using a PID temperature controller, and monitoring with a thermocouple (K type). The errors of their average reaction temperatures were within ±3 °C. The input in the experiments was approximately 150 g, which was fed at different rates of 1.7–3.8 g/min. Table 2 lists the different pyrolysis conditions in each experiment.

2.5. Product analysis

The bio-oil produced was in a heterogeneous state. However, the chemical and physical analyses needed to be carried out in the homogeneous state. After sufficiently stirring the bio-oil, two samples were taken from 10 to 20 vol.% parts of the upper and bottom sections, respectively. The average values of the individual results were taken in triplicate for each analy-

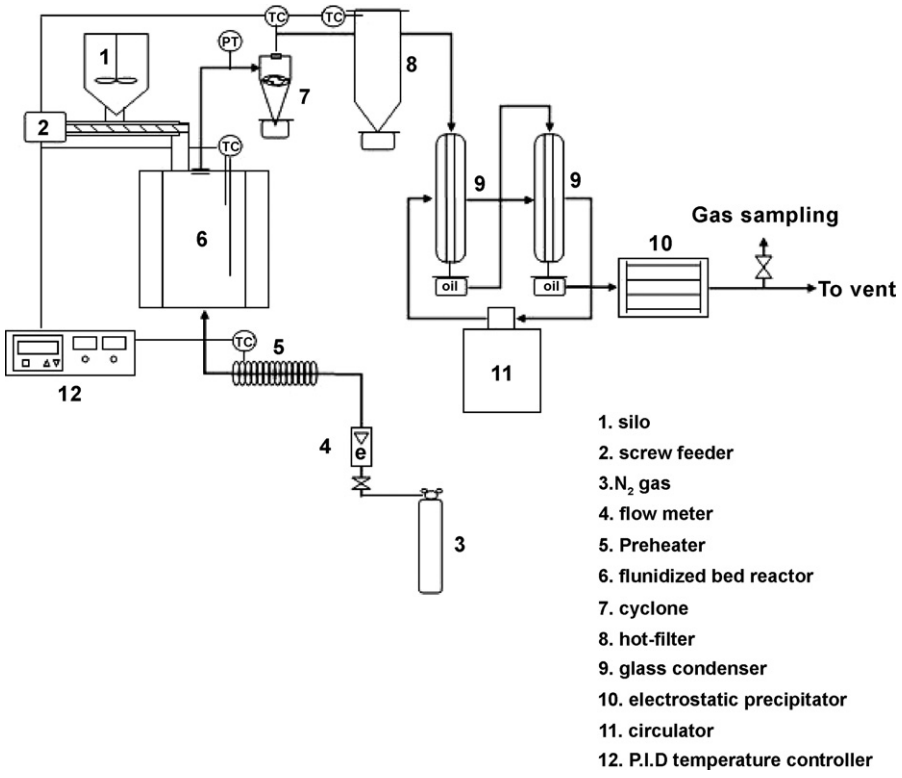

Fig. 1. Schematic diagram of fast pyrolysis apparatus.

sis sample. Since bio-oil contains hundreds of chemicals, the external standard method requires the same number of standard chemicals. This means that accurate quantitative-analysis results of bio-oil are difficult to obtain using the existing gas chromatography equipment. Therefore, the area % of a GC–MS chromatogram can be considered a good approximation because it indicates the amounts of various chemical compounds in bio-oil [11]. In this study, the quantitative and qualitative analyses of bio-oil was performed using GC–MS (HP 5973 *inert*) with a HP-5MS (30 m × 0.25 mm × 0.25 μm) capillary column. Helium was used as the carrier gas. The interpretation of the mass spectra obtained by GC–MS was based on an automatic library search (wiley 7n). The solid content of bio-oil [9] was defined as an acetone-insoluble material retained on a filter (Millipore filtration, 0.1 μm pore size, o.d. 37 mm). The ash content of the bio-oil was calculated by measuring the residues after igniting the bio-oil in a muffle furnace (J-FM2, JISICO) at 850 °C overnight. The higher heating value (Parr, Model 1261) of the bio-oil measured using the KS M 2057 method [12] was compared with the theoretical heating value calculated from Demirbas' equation [13] using the elemental analysis results (Flash EA 1112 series, CE Instruments). The water content of the bio-oil was measured using the ASTM E 203 method [14]. The Karl Fischer titrator (Metrohm 787 KF Titrino) was used, and HYDRANAL Composite 5 K (Riedel-de Haen) and HYDRANAL Working Medium K (Riedel-de Haen) were used as the titration reagent and titration solvent, respectively. The concentration of alkali and alkaline earth metals in the bio-oil was analyzed using inductively coupled plasma atomic-emission spectrophotometry (ICP-AES (138 Ultrace, Jobin Yvon)). The accuracy of the analyses above was <1%. The pyrolysis gases were analyzed using GC-TCD and GC-FID (ACME 6000, Young Lin Instrument Co., Ltd.) using a Carboxen 1000 (15 ft × 1/8 in.) and HP-plot Al_2O_3/KCl column, respectively.

Table 2
Reaction conditions

Parameters	Run1	Run2	Run3	Run4	Run5	Run6	Run7	Run8	Run9	Run10	Run11	Run12
Reaction temperature (°C)	400	450	500	550	450	450	450	450	450	450	450	450
Fluidizing medium[a]	N	N	N	N	N	N	N	N	N	N	P	M
Feed size (mm)	0.7	0.7	0.7	0.7	0.3	1.0	0.7	0.7	0.7	0.7	0.7	0.7
Superficial velocity (cm/s)	1	1	1	1	1	1	0.7	1.3	1	1	1.3	1.3
Feeding rate (g/min)	2.5	2.5	2.5	2.5	2.5	2.5	2.5	2.5	1.7	3.8	2.5	2.5
Input (g)	150	150	150	150	150	150	150	150	150	150	150	150

[a] N: nitrogen, P: product gas, M: mixture gas of oxygen (15 vol.%), and nitrogen (85 vol.%).

3. Results and discussion

3.1. Thermogravimetric analysis

The results of thermogravimetric experiments are expressed as a function of conversion X, which was defined as follows:

$$X = \frac{W_0 - W}{W_0 - W_\infty} \quad (1)$$

where W_0 is the initial mass of the sample, W is the mass of the pyrolyzed sample, and W_∞ is the final residual mass.

Fig. 2 shows the degree of conversion as a function of temperature for the dynamic experiments at heating rates of 5–20 °C/min for Japanese larch in TGA. The early minor weight loss in the samples was attributed to the desorption of moisture as bound water on the surface and the pores of the samples. The decomposition of Japanese larch commenced at 250 °C. The major decomposition of Japanese larch occurred between 300 and 380 °C.

Biomass such as Japanese larch consists of cellulose, hemicellulose, and lignin. Cellulose decomposes over a 30 °C range, typically between 320 and 380 °C [15]. The first weight loss in wood occurs at 300 °C corresponding to the thermal decomposition of hemicellulose and amorphous cellulose [15]. The second occurs at approximately 360 °C due to the decomposition of α-cellulose [15]. Lignin, which constitutes 4–35% of most biomass, has a broad decomposition temperature ranging from 200 to 500 °C, which makes it impossible to define the activation energy for the reaction [15–17].

The differential rate of conversion, dX/dt, was obtained from differential thermogravimetric analysis (DTG) at different heating rates. Fig. 3 shows the typical DTG curves for a heating rate of 5–20 °C/min. A large fraction of Japanese larch was pyrolyzed between 300 and 340 °C, which was attributed to the decomposition of hemicellulose and cellulose. The maximum rates of conversion of the Japanese larch according to the DTG curves occurred at 358, 370, 377, and 382 °C at heating rates of 5, 10, 15 and 20 °C/min, respectively. Alvarez and Vázquez examined the

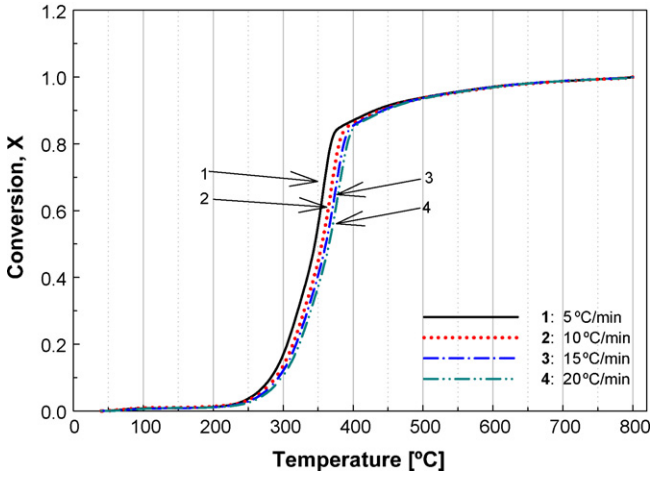

Fig. 2. The effect of pyrolysis rate of Japanese larch at heating rate of 5–20 °C/min: (1) 5 °C/min, (2) 10 °C/min, (3) 15 °C/min, and (4) 20 °C/min.

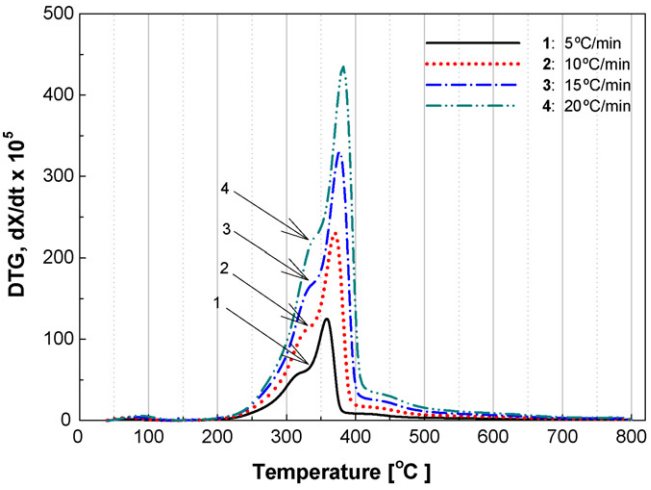

Fig. 3. Variation of the instantaneous reaction rate with temperature at the heating rates of 5–20 °C/min for pyrolysis of Japanese larch.

thermal degradation of cellulose derivatives/starch blends and sisal fibre biocomposites [16]. The sisal fibers showed two DTG peaks, which were attributed to hemicellulose and glucoside linkage depolymerization (300 °C). Thermal decomposition of the α-cellulose was assigned to the peak at 360 °C. In Fig. 3, the first peak for Japanese larch had a small left shoulder at 325 °C at a heating rate of 5 °C/min, which was attributed to the decomposition of hemicellulose. The main peak was assigned to the decomposition of cellulose.

3.2. Kinetic parameters for Japanese larch

Thermogravimetric analysis is widely used to rapidly assess the thermal stability of polymeric materials. The shapes of the TG curves are determined by the kinetic parameters of pyrolysis such as the activation energy, Arrhenius frequency factor and reaction order.

The differential method was used to obtain the pyrolysis kinetic parameters from the thermogravimetric data [18–21]. The rate of conversion, dX/dt, in thermal decomposition was expressed as

$$\left(\frac{dX}{dt}\right) = A\exp\left(-\frac{E}{RT}\right)(1-X)^n \quad (2)$$

The apparent activation energy E, based on Eq. (2) taking the natural logarithm, can be determined from the relationship between ln (dX/dt) and 1/T. During the calculation of activation energy or k value using fitting method, r^2 were over 0.97 with exception of 95% conversion. Fig. 4 shows these data for 5–95% conversion.

The intercept (ln (A·(1–X)^n)) can be calculated from Fig. 4 at each conversion. If the apparent order is fixed to 0, 1, or 2, the pre-exponential factor (A) can obtained by curve fitting of Eq. (3).

$$\ln\left(A(1-X)^n\right) = \ln A + n\ln(1-X) \quad (3)$$

Fig. 5 shows the change in the apparent activation energies as a function of conversion for Japanese larch. The apparent activation energies ranged from 220 to 1009 kJ mol^{-1}, which

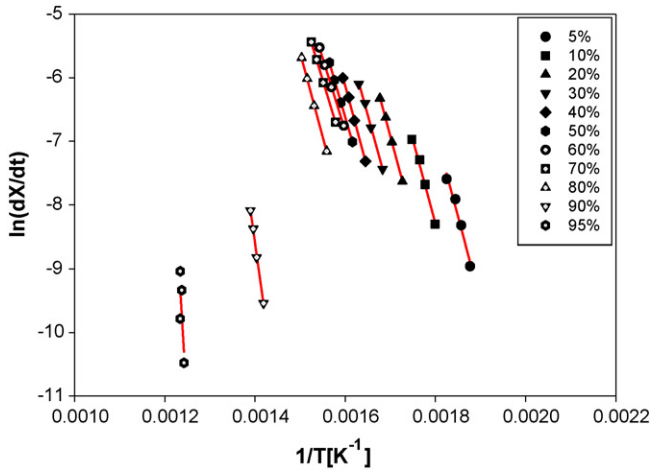

Fig. 4. Application of Eq. (2) with heating rate of 5, 10, 15, and 20 °C/min. The conversion values are: 5–95%.

changed with the level of conversion. The apparent activation energies were almost the same with increasing conversion up to 80%. As shown in the TG curves, hemicellulose and cellulose decomposed below 80% conversion, and the corresponding activation energy ranged from 190 to 220 kJ/mol for the decomposition. Vamvuka et al. examined the pyrolysis characteristics of biomass residual mixtures with lignite [17]. The kinetics of the thermal decomposition was modeled using a scheme consisting of three independent first-order parallel reactions of the main biopolymer components, hemicellulose, cellulose, and lignin. They reported activation energies ranging from 145 to 285 kJ/mol, 90 to 125 kJ/mol, and 30 to 39 kJ/mol for cellulose, hemicellulose, and lignin, respectively. The variation in the apparent activation energy for cellulose showed similar trend to the present data. The higher apparent activation energy at higher conversion appeared to be due to char decomposition.

The pre-exponential factor, which can be obtained from Fig. 4 and Eq. (3), increased with increasing conversion when the reaction order was 0th, 1st, or 2nd (Table 3). The pre-exponential factors ranged from 10^{12} to 10^{20} s^{-1}, at which point the weight

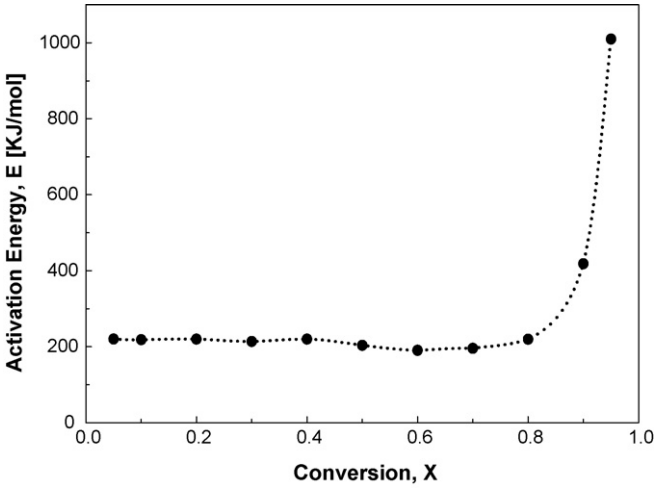

Fig. 5. Calculated activation energies at different conversions for pyrolysis of Japanese larch.

Table 3
Pre-exponential factor for pyrolysis of Japanese larch

Reaction order	Conversion (%)										
	5	10	20	30	40	50	60	70	80	90	95
0th	5.24×10^{17}	8.57×10^{16}	3.35×10^{16}	3.57×10^{15}	5.11×10^{15}	1.36×10^{14}	8.41×10^{12}	1.61×10^{13}	5.78×10^{14}	7.05×10^{26}	1.14×10^{61}
1st	1.05×10^{19}	8.57×10^{17}	1.67×10^{17}	1.19×10^{16}	1.28×10^{16}	2.71×10^{14}	1.40×10^{13}	2.30×10^{13}	7.22×10^{14}	7.83×10^{26}	1.20×10^{61}
2nd	2.10×10^{20}	8.57×10^{18}	8.37×10^{17}	3.96×10^{16}	3.19×10^{16}	5.42×10^{14}	2.34×10^{13}	3.29×10^{13}	9.03×10^{14}	8.70×10^{26}	1.26×10^{61}

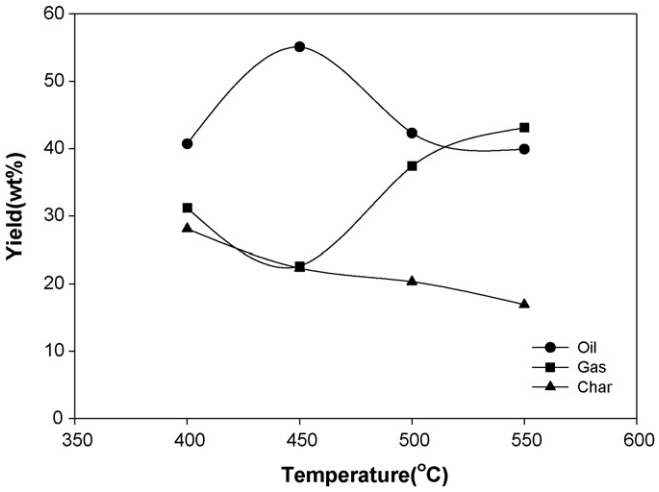

Fig. 6. Behavior of the yield of different pyrolysis as function of the reaction temperature.

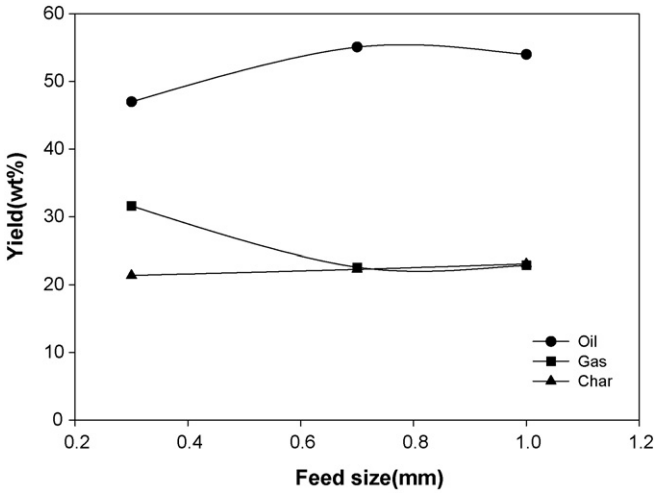

Fig. 7. Behavior of the yield of different pyrolysis as function of the feed size.

loss corresponded to the decomposition of hemicellulose and cellulose in Japanese larch. The pre-exponential factors showed higher values when the conversion was >80% probably because of char decomposition.

3.3. Effect of reaction conditions on product distribution

Fig. 6 shows the product distributions at different reaction temperatures. The bio-oil yield increased to 55 wt% with increasing reaction temperature to 450 °C. The bio-oil yield was decreased at higher temperatures. On the other hand, the gas yield decreased to 22 wt% when the reaction temperature reached 450 °C, and increased to 43 wt% when the reaction temperature was 550 °C. The char yield decreased as the reaction temperature was increased to 550 °C. The reason for the lower bio-oil yield at a lower reaction temperature might be due to the fact that the reaction temperature was not high enough for complete fast pyrolysis, and was similar to slow pyrolysis conditions. On the other hand, the higher gas yield at the higher temperature >450 °C was due to pyrolysis vapors and char being converted into gas through secondary cracking depending on the reaction temperature.

Fig. 7 shows the effect of the feed size on the product distribution. When a particle size <0.3 mm was used, the bio-oil yield decreased to 47 wt% while the gas yield increased to 32 wt%. This result is due to the fact that the smaller sized particles were overheated, which was followed by the conversion of vapors into gas [22]. The particle size had little influence on product distribution at sizes >0.7 mm.

Fig. 8 shows the product distributions at different flow rates. The bio-oil yield increased to 57 wt% depending on the gas flow rate. However, at a low gas flow rate, the gas and char yields increased to 28 and 26 wt%, respectively, while they were not altered at a gas flow rate >3 l/min. This suggests that fluidization is not completely achieved at a lower gas flow rate. Hence, fast pyrolysis could not take place completely [22]. In addition, secondary reactions (i.e., secondary cracking and repolymerization) may occur because the residence time of the vapors in the reactor is longer.

Few studies have reported the effects of the feeding rate on the product distribution. The fluidized bed is generally separated into a dense bed and a suspension bed through a segregation effect. The temperature of the dense bed is higher than that of the suspension bed. Therefore, a higher feeding rate, which will enhance gas flow, can efficiently prevent the vapors from being converted into gas through secondary cracking in the dense bed, resulting in an increase in bio-oil yield [23]. These results show a similar tendency to that reported in the literature. As shown in Fig. 9, it was found that at a high feeding rate, the bio-oil yield increased to 58 wt%. On the other hand, the bio-oil yield decreased at a low feeding rate due to secondary cracking, which was followed by an increase in gas yield.

As shown in Fig. 10, the fluidizing medium had a significant effect on the level of bio-oil production. The bio-oil yield increased up to 64 wt% by using the product gas evolved during pyrolysis as the fluidizing medium. This may be attributed to the

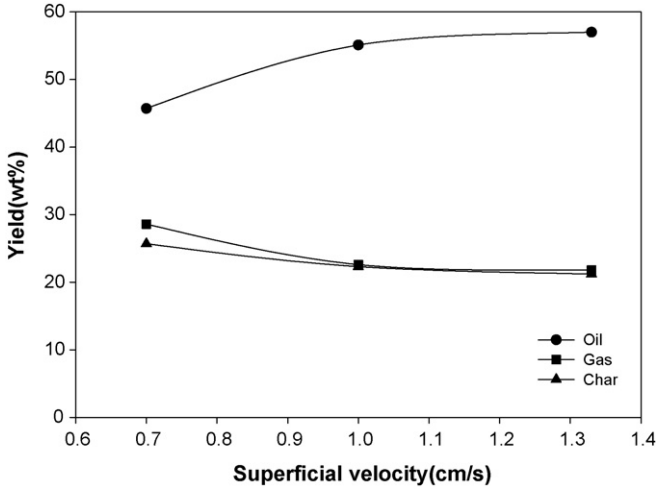

Fig. 8. Behavior of the yield of different pyrolysis as function of the superficial velocity.

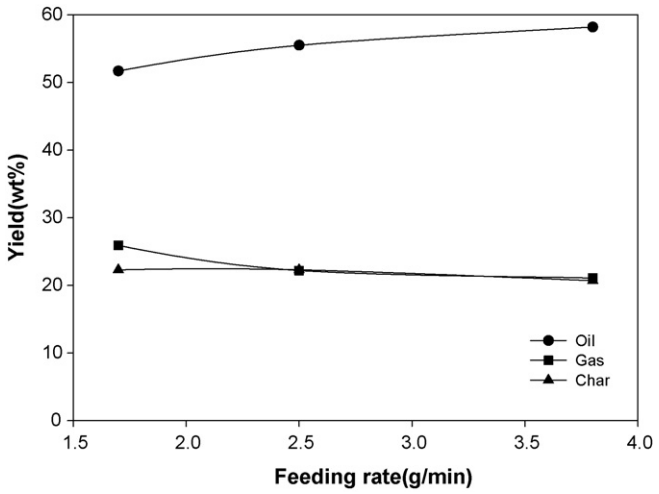

Fig. 9. Behavior of the yield of different pyrolysis as function of the feeding rate.

reaction of product gases such as CO, CO_2, and C_1–C_4 hydrocarbons with pyrolytic vapors in the hot zone in the reactor. In addition, this suggests that the pyrolysis system recirculating the product gas as the fluidizing medium is more effective in the production of bio-oil than an inert gas such as nitrogen. However, a mixture gas containing oxygen decreased the bio-oil yield by approximately 4 wt%. Generally, partial oxidation induces a decrease in the bio-oil yield along with an increase in gas yield due to a partial combustion effect. However, in this study, despite the high oxygen concentration of 15 vol.%, its effect on the bio-oil yield was not as strong as expected.

3.4. Bio-oil

Table 4 lists the results of the chemical and physical analyses of bio-oil obtained through experiment Run10. These results are similar to the typical values reported in the literature [24]. Nitrogen content in bio-oil was significantly low. This indicates that bio-oil might be an environmental friendly fuel. Czernik and Bridgwater showed the typical properties of wood pyrolysis bio-oil and heavy fuel oil [25]. According to them, typical wood pyrolysis bio-oil contains a solid content of 0.2–1.0 wt%. Boucher et al. obtained bio-oil through the vacuum pyrolysis of

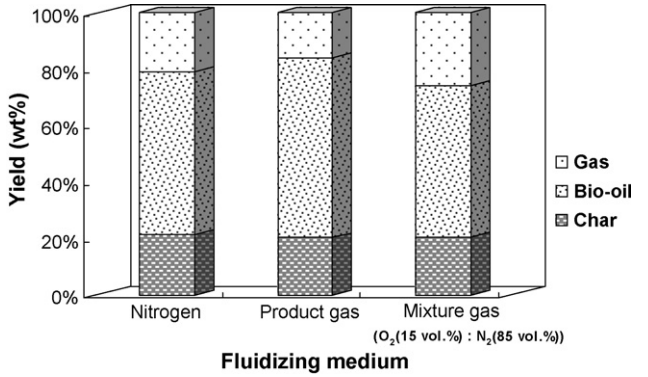

Fig. 10. Behavior of the yield by different fluidizing media.

Table 4
Characteristics of bio-oil obtained through the experiment Run10

Ultimate analysis[a]		Alkali and alkaline earth metals (ppm)	
C	57.0	Na	4.2
H	7.0	Mg	0.1
N	1.8	Ca	2.8
O[b]	34.2	K	<0.1
Water content[b] (wt%)	28.0	Ash content[b] (wt%)	–
Solid content[b] (wt%)	<0.005	pH	2.1
HHV[a,c] (MJ/kg)	22.2	HHV[a,d] (MJ/kg)	23.5

[a] On dry basis.
[b] By difference.
[c] Experiment.
[d] Calculation.

softwood bark residues [26]. This bio-oil had a Na/K/Ca content of 21 ppm, and a solid content of 0.34 wt%. However, in this study, the solid content of bio-oil was 0.005 wt% with the help of a two-staged char removal system with no ash being detected. In addition, the concentrations of alkali and alkaline earth metals were <4.2 ppm. This suggests that better-quality bio-oil was produced, compared with that reported in the literature [25,26]. Bio-oil had a higher heating value (22 MJ/kg), approximately half that of conventional fuel and comparable to that of oxygenated fuels such as methanol, ethanol, and coal [27,28]. In this study, the water content in bio-oils was affected only by the reaction temperature and partial oxidation. The water content in bio-oil increased to 45 wt% with increasing reaction temperature due to thermal cracking. Partial oxidation induced a slight increase in the water content of bio-oil

Table 5
Main compounds identified in bio-oil obtained through the experiment Run10

Compound	Area (%)
Phenol	0.1
2-Methoxy-phenol	6.3
2-Methoxy-4-methyl-phenol	9.6
2-Methyl-phenol	0.7
4-Methoxy-phenol	2.2
2,3-Dimethyl- phenol	1.1
2-Methoxy-4-propyl-phenol	2.9
4-(Ethoxymethyl)-2-methoxy-phenol	0.7
2-Methoxy-4-vinylphenol	3.7
1,4-Dimethoxy-benzene	0.4
1,2-Dimethoxy-4-methyl-benzene	0.2
2-Methoxy-benzeneethanol	4.9
2-Hydroxy-3-methyl-2-cyclopenten-1-one	2.3
2-Cyclopenten-1-one	0.4
2-Methyl-2-cyclopenten-1-one	0.6
2(5H)-furanone	1.8
5-Methyl-2(3H)-furanone	3.9
2-Furancarboxaldehyde	3.3
5-Methyl-2-furancarboxaldehyde	1.3
Eugenol	2.9
Iso-eugenol	11.1
4-Hydroxy-3-methoxy-Benzaldehyde	0.6
1-(2-Furanyl)-ethanone	0.2
1-Methoxy-1,3-cyclohexadiene	0.2
1,6-Anhydro-beta-D-glucopyranose	5.3
Acetic acid	1.5

Table 6
Composition of gas products from different pyrolysis conditions

Composition (wt%)	Run1	Run2	Run3	Run4	Run5	Run6	Run7	Run8	Run9	Run10	Run11	Run12
CO	36.2	42.8	46.8	56.0	41.4	42.1	42.0	40.9	40.7	41.1	41.0	34.3
CO_2	59.6	48.0	40.0	25.4	50.1	48.8	48.2	50.1	49.9	50.0	51.5	62.2
C_1–C_4	4.2	9.1	13.2	18.6	8.5	9.1	9.8	8.9	9.4	8.9	7.5	3.5

to 38 wt%, which is likely to be due to either gasification or decomposition of large molecules through partial combustion (data not shown). However, the water content in bio-oil under the other experimental conditions ranged from 28 to 30 wt%. Table 5 shows the chemical composition of the bio-oil obtained through experiment Run10. The major compounds in the bio-oil were phenolics, including cresols, guaiacols, eugenols, and their derivatives, ketones, and aldehydes. After fractionating, these compounds may be used as a feedstock for useful chemicals. However, aromatic hydrocarbons such as benzene and naphthalene derivatives, were formed only at 550 °C (data not shown). The partial oxidation decreased the phenolics yield (data not shown). The decreases in the amount of low molecular weight phenolics, such as phenol and alkylated phenols, were lower than high molecular weight molecules. This was attributed to the cracking of large molecular phenolics followed by partial conversion into phenol and alkylated phenols.

3.5. Gas

The gas products were analyzed quantitatively using GC-TCD and GC-FID. As shown in Table 6, the main gas products were composed of CO, CO_2, and C_1–C_4 hydrocarbons, and hydrogen was negligible as less than 0.2 wt%. It was found that a high reaction temperature leads to a high proportion of CO and C_1–C_4 hydrocarbons and a low proportion of CO_2. This was attributed to the secondary cracking of volatiles, followed by the reduction of CO_2 at higher reaction temperatures to CO and CH_4 [29]. In particular, the increase in the content of CO and C_1–C_4 hydrocarbons with high caloric values suggests that the gas products can be used as energy sources for the pyrolysis process or other applications. For partial oxidation, the level of CO_2 increased due to the combustion effect, whereas the amount of CO and C_1–C_4 hydrocarbons decreased. The gas composition was rarely influenced by each pyrolysis condition except for the reaction temperature and partial oxidation.

4. Conclusions

As a result of a kinetic investigation into Japanese larch pyrolysis, the TG curves of Japanese larch exhibited a weight loss regime, completing the decomposition between 250 and 380 °C. The apparent activation energies ranged from 220 to 1009 kJ mol^{-1}, which changed with the level of conversion. The pre-exponential factor assuming an overall 0th, 1st, and 2nd order reaction ranged from 10^{12} to 10^{20} s^{-1} for the decomposition of hemicellulose and cellulose in Japanese larch. The optimal reaction temperature for the production of bio-oil was 450 °C. A smaller feed size had a negative influence on the production of bio-oil. The bio-oil yields were increased gradually along with increase of the flow rate and the feeding rate but these did not significantly affect the bio-oil yields. The use of the product gas as a fluidizing medium gave the highest bio-oil yield, whereas during pyrolysis, the introduction of oxygen had a slight negative effect on the bio-oil yield. In addition, high-quality bio-oil containing <0.005 wt% solid, no ash, and low concentrations of alkali and alkaline earth metals, could be produced through the introduction of a two-staged removal system. With the exception of the reaction temperature and partial oxidation, the other pyrolysis conditions did not have a significant effect on the chemical and physical characteristics of the bio-oil product.

Acknowledgment

This study was supported by the Ministry of Environment in Korea as “The Eco-technopia 21 Project”.

References

[1] IEA Bioenergy, IEA Bioenergy Task 34: biomass pyrolysis 2007.
[2] IEA Bioenergy, benefits of bioenergy, IEA Bioenergy: ExCo 2005.
[3] A.E. Pütün, N. Özbay, E.P. Önal, E. Pütün, Fixed-bed pyrolysis of cotton stalk for liquid and solid products, Fuel. Process. Technol. 86 (2005) 1207–1219.
[4] A.E. Pütün, E. Apaydm, E. Pütün, Rice straw as a bio-oil source via pyrolysis and steam pyrolysis, Energy 29 (2004) 2171–2180.
[5] F. Ates, E. Pütün, A.E. Pütün, Fast pyrolysis of sesame stalk: yields and structural analysis of bio-oil, J. Anal. Appl. Pyrolysis 71 (2004) 779–790.
[6] S. Sensöz, I. Demiral, H.F. Gercel, Olive bagasse (Olea europea L.) pyrolysis, Bioresour. Technol. 97 (2006) 429–436.
[7] J.F. Gonzalez, A. Ramiro, C.M. Gonzalez-Garcia, J. Ganan, J.M. Encinar, E. Sabio, J. Rubiales, Pyrolysis of almond shells. Energy applications of fractions, Ind. Eng. Chem. Res. 44 (2005) 3003–3012.
[8] A. Demirbas, Effect of initial moisture content on the yields of oily products from pyrolysis of biomass, J. Anal. Appl. Pyrolysis 71 (2004) 803–815.
[9] A. Oasmaa, C. Peacocke, A Guide to Physical Property Characterization of Biomass-derived Fast Pyrolysis Liquids, VTT Publication, Espoo, 2001.
[10] A.R. Abrahamsen, D. Geldart, Behaviour of gas-fluidized beds of fine powders part I. Homogeneous expansion, Powder Technol. 26 (1980) 35–46.
[11] M.C. Samolada, A. Papafotica, I.A. Vasalos, Catalyst evaluation for catalytic biomass pyrolysis, Energy Fuels 14 (2000) 1161–1167.
[12] Korea Standards Association, Crude petroleum and petroleum products—determination and estimation of heat of combustion, KS M 2057, Seoul, 2006.
[13] A. Demirbas, Calculation of higher heating values of biomass fuels, Fuel 76 (1997) 431–434.
[14] American Society for Testing and Materials, Standard Test Method for Water Using Volumetric Karl Fischer Titration, ASTM E 203, West Coushohocken (2001).

[15] S. Gaur, T.B. Reed, An Atlas of Thermal Data for Biomass and Other Fuels, National Renewable Energy Laboratory, 1994.
[16] V.A. Alvarez, A. Vázquez, Thermal degradation of cellulose derivatives/starch blends and sisal fibre biocomposites, Polym. Degrad. Stabil. 84 (2004) 13–21.
[17] D. Vamvuka, E. Kakaras, E. Kastanaki, P. Grammelis, Pyrolysis characteristics and kinetics of biomass residuals mixtures with lignite, Fuel 82 (2003) 1949–1960.
[18] S.S. Kim, S.D. Kim, Pyrolysis characteristics of polystyrene and polypropylene in a stirred batch reactor, Chem. Eng. J. 98 (2004) 53–60.
[19] S.S. Kim, J.K. Jeon, Y.K. Park, S.D. Kim, Thermal pyrolysis of fresh and waste fishing nets, Waste Manage. 25 (2005) 811–817.
[20] T.H. Liou, F.W. Chang, J.J.L. Lo, Pyrolysis kinetics of acid-leached rice husk, Ind. Eng. Chem. Res. 36 (1997) 568–573.
[21] H.L. Friedman, Kinetics of thermal degradation of char-forming plastics from thermogravimetry. Application to a phenolic plastic, J. Polym. Sci. 6 (1963) 183–195.
[22] M.N. Islam, R. Zailani, F.N. Ani, Pyrolytic oil from fluidised bed pyrolysis of oil palm shell and itscharacterisation, Renew. Energy 17 (1999) 73–84.
[23] Z. Luo, S. Wang, K. Cen, A model of wood flash pyrolysis in fluidized bed reactor, Renew. Energy 30 (2005) 377–392.
[24] A.V. Bridgwater, D. Meier, D. Radlein, An overview of fast pyrolysis of biomass, Org. Geochem. 30 (1999) 1479–1493.
[25] S. Czernik, A.V. Bridgwater, Overview of applications of biomass fast pyrolysis oil, Energy Fuels 18 (2004) 590–598.
[26] M.E. Boucher, A. Chaala, C. Roy, Bio-oils obtained by vacuum pyrolysis of softwood bark as a liquid fuel for gas turbines. Part I: properties of bio-oil and its blends with methanol and a pyrolytic aqueous phase, Biomass Bioenergy 19 (2000) 337–350.
[27] A. Demirbas, Biomass resource facilities and biomass conversion processing for fuels and chemicals, Energy Convers. Manage. 42 (2001) 1357–1378.
[28] K. Raveendran, A. Ganesh, Heating value of biomass and biomass pyrolysis products, Fuel 75 (1996) 1715–1720.
[29] A. Demirbas, Gaseous products from biomass by pyrolysis and gasification: effects of catalyst on hydrogen yield, Energy Convers. Manage. 43 (2002) 897–909.